

On Parameterizing PEM Fuel Cell Models

Alireza Goshtasbi, Jixin Chen, James R. Waldecker, Shinichi Hirano, Tulga Ersal*

Abstract—A methodology for parameterizing polymer electrolyte membrane (PEM) fuel cell models is presented. The procedure starts by optimal experimental design (OED) for parameter identification. This is done by exploring output sensitivities to parameter variations in the space of operating conditions. Once the optimal operating conditions are determined, they are used to gather synthetic experimental data. The synthetic data are then used to identify 7 model parameters in a step-by-step procedure that involves grouping the parameters for identification based on the preceding sensitivity analysis. Starting from the kinetic region of the polarization curve and continuing with the ohmic and mass transport regions, the parameters are identified in a cumulative fashion using a gradient-based nonlinear least squares algorithm. The impact of the OED for parameter identification is explored by comparing the results with another set of synthetic data obtained by Latin Hypercube Sampling (LHS) of the operating space. The results indicate improved identification with OED compared to LHS and point to the utility of the systematic approach, presented herein, for identifying the parameters of PEM fuel cell models.

I. INTRODUCTION

As PEM fuel cells draw near a more widespread use in the automotive industry, developing models for the fuel cell stacks becomes more critical. Fuel cell models can be used to understand the details of various transport phenomena inside each individual cell, study different aspects of cell degradation, and develop on-board model-based monitoring and control methodologies for improved performance and durability [1]. Therefore, having representative models for each application and proper model parameterization are of great significance. Even though a number of mathematical models are available in the literature for fuel cell systems with different levels of fidelity, model parameterization is a topic that has remained relatively understudied. Having identified this as a crucial gap in the fuel cell literature, here we report on our first steps to systematically address this challenge, utilizing a recently developed model of PEM fuel cells.

The topic of model parameterization for electrochemical energy systems has gained some popularity in recent years, mostly due to the battery research community. In particular, the question of parameter identifiability in various lithium ion battery models has been investigated using the Fisher information matrix [2], [3], [4], [5] and bounds on the parameter estimates have been investigated [6]. More recently, there has been a shift towards optimally designing experiments

for the purpose of parameter identification by maximizing some metric of identifiability. Zhang et al. designed optimal experiments based on the sensitivity of the terminal voltage and shell temperature to parameter variations [7]. Others have mostly resorted to maximizing a scalar metric of the Fisher information matrix for this purpose [8], [9], [10]. Overall, the battery literature offers promising approaches for systematic model parameterization.

In the fuel cell literature, the problem of parameterizing mathematical models is mostly treated as material characterization. That is, the parameters are usually obtained by often costly ex-situ component characterization methods and the models are expected to reproduce in-situ experimental data from a fuel cell stack. This not only requires being able to take the cells apart and investigate their components individually, but also often results in the models' representation capabilities not being fully utilized and most literature citing only qualitative agreement with experimental data as a validation of the models (e.g. see [11]). There are some exceptions to this general trend, the most notable of which are perhaps the works of Dobson et al. [12] and Carnes et al. [13], who use nonlinear least squares to identify model parameters. Nevertheless, such optimization based parameterization approaches are not common in the fuel cell community, which is most likely due to the significant computational requirements of many of the available fuel cell models that inhibit the use of these techniques.

Recognizing the need for systematic model parameterization approaches, here we use a model of PEM fuel cell that we have recently developed for online estimation [14], [15], and propose a methodology for identifying its parameters. In particular, we start by optimally designing the experiments with the goal of parameter identification in mind. This is then followed by a procedure that involves grouping the parameters based on their sensitivity and identifying the parameter groups in three steps using synthetic experimental data; i.e. data obtained through simulations. The results are compared against those obtained with experimental design using LHS. Moreover, we compare the results of the systematic procedure with those of identifying all of the parameters in a single optimization problem. The OED and systematic procedure proposed here, which are independent of the model in use and constitute the major contributions of this paper, differentiate this work from prior art [12], [13].

The rest of the paper is organized as follows. We briefly describe the OED adapted from [7] in Section II. The three-step parameter identification procedure is explained in Section III. Identification results and discussions are provided in Section IV, followed by concluding remarks in Section V.

* Corresponding author (tersal@umich.edu)

Alireza Goshtasbi and Tulga Ersal are with the Department of Mechanical Engineering, University of Michigan, Ann Arbor, MI.

Jixin Chen, James Waldecker, and Shinichi Hirano are with the Fuel Cell Research, Ford Motor Company, Dearborn, MI.

TABLE I
MODEL PARAMETERS TO BE IDENTIFIED

Parameter	Description
ω	Energy parameter for Temkin isotherm [J/mol]
α_{ca}	ORR* transfer coefficient [-]
$i_{0,ca}$	ORR exchange current density [A/cm ²]
δ_{mb}	Membrane thickness [μm]
R_{ohm}	Ohmic resistance of cell layers [Ω · cm ²]
$\delta_{GDL,an}$	Anode GDL [†] thickness [μm]
$\delta_{GDL,ca}$	Cathode GDL thickness [μm]
$K_{abs,MPL}$	MPL [‡] absolute permeability [m ²]

* Oxygen Reduction Reaction
† Gas Diffusion Layer
‡ Microporous Layer

II. OPTIMAL EXPERIMENTAL DESIGN (OED) FOR PARAMETER IDENTIFICATION

A. Model Parameters to be Identified

The model used in this work is a computationally efficient pseudo-2D model of the PEM fuel cell that solves, along the flow channels, the heat and mass transport problems across the thickness of a single cell. The details of this model have been presented previously [14], [15] and are omitted here for brevity. The model has many geometrical, kinetic, and thermodynamic parameters as well as fitting coefficients used to fit some of the sub-models to ex-situ experimental characterization data. For the demonstration purposes of this paper, we have selected 8 parameters for identification. The selected parameters are provided in Table I along with their descriptions.

B. Sensitivity Analysis and Parameter Identifiability

As a first step towards optimally designing experiments for parameter identification, the sensitivity of the model outputs to parameter variations should be studied. In this work, we assume that only voltage measurements are available. Therefore, we start by investigating the sensitivity of the voltage prediction to variations in the selected parameters described above. However, it is important to note that other signals, such as high frequency resistance, may be easily measured in a fuel cell system with standard equipment. Therefore, these peripheral signals can be used to further improve the identification process and render more of the model parameters identifiable. Nevertheless, identification based on voltage measurement alone serves as a good starting point to develop a systematic framework.

The sensitivity analysis is conducted by discretizing the space of operating conditions as follows:

$$\begin{aligned} \text{Pressure} &\in \{1.5, 2.0, 2.5, 3.0\} \text{ bar} \\ \text{Stoichiometric Ratio} &\in \{1.5, 2.5, 3.5\} \\ \text{Relative Humidity} &\in \{30, 60, 90\}\% \\ \text{Temperature} &\in \{60, 70, 80\}^{\circ}\text{C} \end{aligned}$$

The above discretization results in 108 unique operating conditions using a full factorial design. The parameter sensitivities at each of these conditions are investigated by perturbing each parameter from its nominal value within some bounds. In particular, for every parameter, 9 simulated polarization curves are obtained at each operating condition; one baseline curve with the nominal parameter value, and 8 perturbed

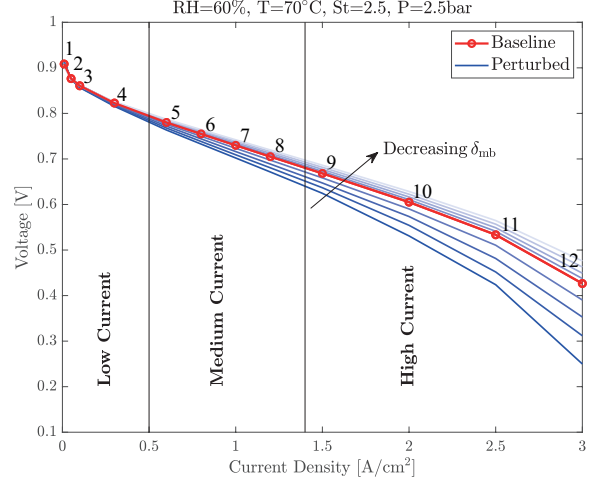


Fig. 1. Effect of variations in δ_{mb} on the polarization curve (the operating conditions are given on top of the figure). Simulated voltages for 12 points are obtained for each polarization curve.

curves with the perturbed parameter values as illustrated in Fig. 1. The resulting polarization curve is divided into 3 regions: low, medium, and high current density, representing the kinetic, ohmic, and mass transport (MT) regions of the curve, respectively. 4 points are simulated in each region of the curve for each parameter set. The sensitivity of the output voltage to parameter variations in each region is obtained by computing the average standard deviation of simulated voltage values among the 9 polarization curves:

$$\begin{aligned} S_{\text{Kinetic}} &= \text{mean}(\sigma_1, \sigma_2, \sigma_3, \sigma_4), \\ S_{\text{Ohmic}} &= \text{mean}(\sigma_5, \sigma_6, \sigma_7, \sigma_8), \\ S_{\text{MT}} &= \text{mean}(\sigma_9, \sigma_{10}, \sigma_{11}, \sigma_{12}), \end{aligned} \quad (1)$$

where σ_i denotes the standard deviation of the i -th point on the 9 simulated polarization curves. More specifically:

$$\sigma_i = \sqrt{\left[\sum_{j=1}^9 (V_{i,j} - \frac{1}{9} \sum_{k=1}^9 V_{i,k}) \right]^2 / 8}, \quad i = \{1, 2, \dots, 12\}, \quad (2)$$

where $V_{i,j}$ is the i -th voltage value on the j -th polarization curve (Fig. 1).

Once the sensitivities are calculated, we can determine parameter identifiability. Here, we use the approach adopted by Zhang et al. [7] and specify a sensitivity threshold, below which a parameter is deemed unidentifiable. In particular, any parameter with a maximum sensitivity below 0.006 is labeled unidentifiable and removed from the identification process. In this work, only $K_{abs,MPL}$ was determined to be unidentifiable. Other parameters are labeled as having “High Sensitivity” if their average sensitivity is above 0.01, and “Low Sensitivity” otherwise. Alternatively, one can group the parameters and study the linear dependence between them based on the QR factorization of the sensitivity matrix [10], [16]. Nevertheless, we use the sensitivity thresholding as a first step in this paper due to its simplicity. The complete results of the sensitivity analysis are provided in Table II.

TABLE II
PARAMETER SENSITIVITIES

Parameter	S_{\max}	S_{avg}	Sensitivity	Group
ω	0.0536	0.0223	High	Kinetic
α_{ca}	0.1578	0.1009	High	Kinetic
$i_{0,\text{ca}}$	0.1620	0.1101	High	Kinetic
δ_{mb}	0.1327	0.0238	High	Ohmic
R_{ohm}	0.0222	0.0074	Low	Ohmic
$\delta_{\text{GDL,an}}$	0.0198	0.0011	Low	MT
$\delta_{\text{GDL,ca}}$	0.0509	0.0066	Low	MT
$K_{\text{abs,MPL}}$	0.0045	0.00003	Insensitive	N/A

Another important step is to group the parameters that should be identified together using data from a specific region of the polarization curve. The goal of this step is to find regions on the polarization curve that are only sensitive to variations in a specific subset of the parameters. Doing so will allow us to develop a step-by-step identification process, which can begin by identifying a subset of parameters in a region that is not significantly affected by the errors in the other, yet unidentified parameters.

Accordingly, we define three groups aligned with the three regions that we have previously specified on the polarization curve (Fig. 1): the first parameter group consists of those parameters that are identifiable in the low current density region of the polarization curve, while the second and third groups include the parameters that become identifiable at medium and high current densities, respectively. The general idea is that the voltage sensitivity to parameter variations typically increases as the current is increased. Therefore, it is helpful to start the identification process by only using the data at low current densities and as our confidence in the parameter estimates increases, move along the polarization curve to higher currents and identify the remaining parameters. It is conceivable that there is some benefit in increasing the number of parameter groups, especially if more parameters are to be identified.

In this work, the grouping is done based on the average voltage sensitivities in each region of the polarization curve. As can be seen in Fig. 2, parameters whose average sensitivity in a particular region of the polarization curve is above a certain threshold, belong to the same group. Therefore, three parameters can be identified using low current or kinetic region data ($\omega, \alpha_{\text{ca}}, i_{0,\text{ca}}$), two parameters can be identified using medium current or ohmic region data ($\delta_{\text{mb}}, R_{\text{ohm}}$), and two other parameters can only be identified using high current or mass transport region data ($\delta_{\text{GDL,an}}, \delta_{\text{GDL,ca}}$).

As a final note, we acknowledge that these sensitivity results are local and depend on the nominal parameter values used in this work. There is no doubt that with a global sensitivity analysis the proposed framework will be more robust. However, the computational cost of such an analysis renders it infeasible at this point.

C. Selection of Optimal Experiments for Parameter Identification

With $K_{\text{abs,MPL}}$ removed from the identification process due to its low sensitivity, there remains 7 parameters to

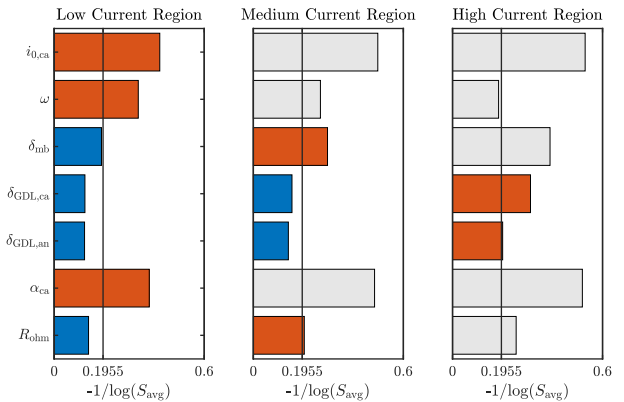


Fig. 2. Average voltage sensitivities to parameter variations in various regions of the polarization curve. Longer bars show higher sensitivities. Red bars denote parameters that satisfy the sensitivity threshold and can be identified using data in the specified region. Blue bars denote parameters that are yet to be grouped, and gray bars show parameters that are already labeled as belonging to a group. The sensitivity threshold for parameter grouping is $0.1955 = -1/\log(0.006)$, i.e., the sensitivity threshold is the same as that used to determine identifiability of parameters.

be identified. Here, we seek to find the optimal operating conditions that maximize identifiability of these parameters with a small number of experiments. This is especially important, since some operating conditions may render a parameter unidentifiable, while others can result in high sensitivity to the parameter variations. Fig. 3 illustrates this by plotting the normalized voltage sensitivities to variations in δ_{mb} at different operating conditions. It can be seen that generally drier conditions, higher temperatures, and higher flow rates are more suitable for identification of this parameter. While this observation is rather intuitive for the membrane thickness, such simple physical insights are rarely available for other parameters due to the complex interactions between various transport phenomena.

The process for selecting optimal experiments for parameter identification is as follows:

- 1) Specify the Best Conditions for Identification (BCI) [7] of each parameter. This can be done by ranking the operating conditions based on the particular parameter's sensitivity and choosing the corresponding top 10 operating conditions, which yields a total of 70 BCIs (e.g. in Fig. 3, the three largest dots indicate three BCIs for δ_{mb}).
- 2) Remove any repeated operating condition from the list.
- 3) Find the smallest subset of these operating conditions that includes at least one BCI for each parameter and maximizes the weighted sum of the sensitivities. The weights are used to prioritize maximizing the sensitivity of parameters with lowest sensitivity.

The last step can be formulated as an integer program:

$$\begin{aligned}
 & \underset{n_i}{\text{minimize}} && -\mathbf{w}^T \mathbf{S}_\theta \\
 & \text{subject to} && \mathbf{S}_{\theta,j} = \sum_{i=1}^{N_{\text{tot}}} n_i b_{i,j} s_{i,j} \neq 0, \\
 & && \sum_{i=1}^{N_{\text{tot}}} n_i = N, \\
 & && n_i \in \{0, 1\},
 \end{aligned} \tag{3}$$

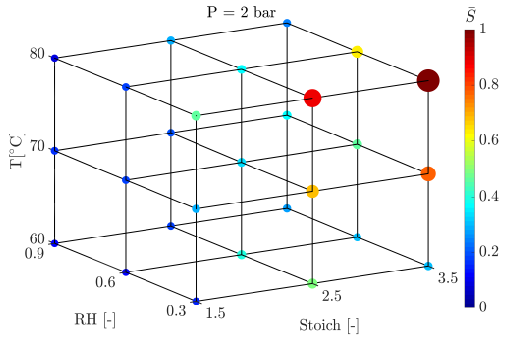


Fig. 3. Normalized voltage sensitivity to variations in δ_{mb} (larger dots indicate higher sensitivity).

TABLE III
OPTIMAL EXPERIMENTS FOR PARAMETER IDENTIFICATION

P [bar]	T [°C]	Stoich	RH	Parameter BCIs
2.5	80	2.5	90	$\delta_{GDL,an}, \delta_{GDL,ca}$
1.5	80	3.5	30	$i_{0,ca}, \delta_{mb}, R_{ohm}$
1.5	60	1.5	30	α_{ca}
3.0	80	3.5	90	ω

where w is a weighting vector used to promote the parameters with low sensitivity, $S_\theta \in \mathbb{R}^{7 \times 1}$ is a vector of sensitivities, N_{tot} is the total number of operating conditions from which a subset of size N is to be selected, $b_{i,j}$ is an indicator function that is identity if the i -th operating condition is a BCI for the j -th parameter, and n_i 's are the optimization variables that determine whether or not an operating condition should be included in the experiments. One should note that if two BCIs for a parameter are included in the selected subset, only the largest sensitivity should be used in forming S_θ . This integer program may be relaxed into a convex program [10]. However, this particular instance of the problem can be readily solved by simply testing all of the possibilities due to the small size of the search space. It is thus determined that at least 4 experiments are needed to cover BCIs for all 7 parameters. Furthermore, we use a weight of 10 for parameters with low sensitivity and a weight of 1 for those with high sensitivity. This results in the particular choice of operating conditions that is presented in Table III.

D. Experimental Design Using LHS

To investigate the utility of OED, another set of experiments are designed by taking Latin hypercube samples of the space of operating conditions. The resulting experimental designs are given in Table IV.

III. THE 3-STEP PARAMETER IDENTIFICATION METHOD

A. Identification Steps

After the sensitivity analysis is conducted and parameters are grouped accordingly, the optimal experiments specified in Section II-C can be used for the purpose of parameter identification. In this paper, we use the optimal experiments to generate synthetic data using simulations with a known set of parameters. The parameters under investigation are then

TABLE IV EXPERIMENTAL DESIGN USING LHS			
P [bar]	T [°C]	Stoich	RH
2.2	63.7	2.9	63.7
1.6	68.5	1.8	68.5
2.7	71.9	3.2	71.9
2.5	78.7	2.4	78.7

perturbed from their nominal values and treated as unknown parameters to be identified.

The identification algorithm has three steps as follows:

- 1) Parameters in the first group are identified using low current density data in the kinetic region. All the other parameters are kept at their initial value during this step and are not updated.
- 2) Parameters in the second group are identified using medium current density data in the ohmic region. It is important to note that parameters in the third group are kept constant at their initial value during this step, while those in the first group that were identified earlier, are allowed to vary in a smaller region, i.e., the search space for the parameters in the first group is contracted.
- 3) The third group of parameters is identified using high current density data in the mass transport region. During this step, parameters in the first and second groups are allowed to vary, but their respective search space is contracted. In particular, the search space for first group of parameters is even smaller than their search space in the second step of the algorithm.

Allowing previously identified parameters to be further refined as the algorithm moves along the polarization curve is critical for successful identification. This is due to the fact that in most cases parameter sensitivities increase with current density, and so does their identifiability. Therefore, we can obtain more accurate parameter values by allowing for such cumulative fitting [7], [10]. Finally, as we move to higher currents, we disregard lower current data points in this work. Alternatively, one may use low current data at later stages of the identification algorithm along with larger weights for the higher current measurements (i.e. weighted least squares).

B. Parameter Scaling

Proper scaling of the parameters is also critically important, especially if first-order numerical algorithms are to be utilized. Similar to [10], here we use min-max scaling, where parameters are scaled either linearly or logarithmically depending on their respective range. Parameter ranges and the scaling method are given in Table V.

This yields a set of parameters that vary between 0 to 1. This parameter scaling is repeated after each step of the algorithm is completed and the search space for the identified parameters is contracted. In particular, after the first step of the algorithm, the search space for the first group of parameters is limited to ± 0.2 of the identified normalized parameter values. As we move to the second step of the

TABLE V
PARAMETER BOUNDS AND SCALING

Parameter	Lower Bound	Upper Bound	Scaling
ω	10^2	10^5	Logarithmic
α_{ca}	0.4	1.0	Linear
$i_{0,ca}$	10^{-9}	10^{-5}	Logarithmic
δ_{mb}	8	30	Linear
R_{ohm}	10^{-4}	10^{-2}	Logarithmic
$\delta_{GDL,an}$	140	240	Linear
$\delta_{GDL,ca}$	140	240	Linear

algorithm, the first group of parameters are again scaled to lie between 0 and 1. As the algorithm proceeds to later stages, this search space is shrunken further. For instance, during the third step, the search space for the first group of parameters is limited to ± 0.1 of the normalized parameter values identified in the second step. This successive shrinking of the search space enables a more accurate parameter identification. Nevertheless, one has to be careful not to shrink the search space too much after each step to make sure that it includes the optimal value. One may use the confidence intervals as a more robust guideline for shrinking the search space for the identified parameters.

C. Nonlinear Least Squares Algorithm

Any nonlinear least squares algorithm may be used for parameter identification in conjunction with the steps laid out earlier. Here we use the Levenberg-Marquardt algorithm that hybridizes Gauss-Newton with gradient descent updates [17]. This algorithm is chosen to demonstrate the utility of OED in improving the gradients used in a gradient-based method. However, we note that in practice when the number of parameters to be identified is large and the cost function is rather noisy, both of which are common for models of electrochemical energy systems, a hybrid approach utilizing both gradient-free and gradient-based algorithms may be the best choice.

D. Calculation of Confidence Intervals

The 95% confidence intervals (CI) for parameter estimates can be calculated by [18]:

$$\hat{\boldsymbol{\theta}} - t_{(0.95,n-p)}\sigma_{\boldsymbol{\theta}} \leq \boldsymbol{\theta} \leq \hat{\boldsymbol{\theta}} + t_{(0.95,n-p)}\sigma_{\boldsymbol{\theta}}, \quad (4)$$

where $t_{(0.95,n-p)}$ is the critical value for t-distribution with $n - p$ degrees of freedom, with n being the number of data points and p being the number of estimated parameters. Moreover:

$$\sigma_{\boldsymbol{\theta}} = \sqrt{\mathbf{R}^2 \text{diag}([\mathbf{J}^T \mathbf{J}]^{-1})}, \quad (5)$$

where \mathbf{J} is the Jacobian calculated at the final parameter estimates and \mathbf{R} is the scaled vector of residuals. In particular:

$$\mathbf{J} = \frac{\partial \mathbf{E}}{\partial \boldsymbol{\theta}} \Big|_{\boldsymbol{\theta}=\hat{\boldsymbol{\theta}}}, \text{ and } \mathbf{R} = \frac{\|\mathbf{E}\|}{\sqrt{n-p}}, \quad (6)$$

where $\boldsymbol{\theta}$ denotes the vector of parameters, $\hat{\boldsymbol{\theta}}$ denotes the final parameter estimates, and \mathbf{E} denotes the vector of residuals, i.e., the error between the model predictions and measurements.

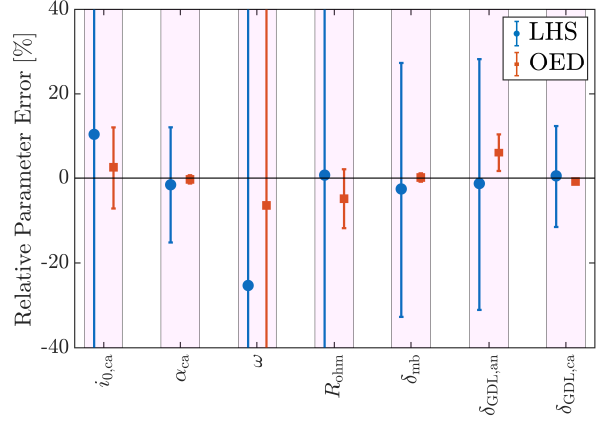


Fig. 4. Relative error in parameter estimates and their corresponding 95% confidence intervals using OED and LHS design. Note that for the LHS design the confidence intervals of some of the parameters extend beyond the relative error range shown.

TABLE VI
IDENTIFICATION RESULTS USING OED

Parameter	True Value	Estimated Value	95% CI
ω	1000	936.4	1010
α_{ca}	0.7	0.698	0.0067
$i_{0,ca}$	3×10^{-7}	3.07×10^{-7}	2.88×10^{-8}
δ_{mb}	15	15.02	0.14
R_{ohm}	8.0×10^{-3}	7.6×10^{-3}	5.5×10^{-4}
$\delta_{GDL,an}$	190	201.5	8.36
$\delta_{GDL,ca}$	190	188.5	1.23

IV. RESULTS AND DISCUSSION

We start the identification process with perturbed parameter values. Specifically, the initial point for the normalized parameter values is given by:

$$\bar{\boldsymbol{\theta}}_0 = [\bar{\omega}, \bar{\alpha}_{ca}, \bar{i}_{0,ca}, \bar{\delta}_{mb}, \bar{R}_{ohm}, \bar{\delta}_{GDL,an}, \bar{\delta}_{GDL,ca}]^T \\ = [0.5, 0.3, 0.75, 0.5, 0.7, 0.7, 0.7]^T$$

This particular set was chosen arbitrarily from various parameter sets available in the literature that yield reasonable polarization curves. The algorithm presented in Section III is then used to identify these parameters using synthetic data generated with both the optimal conditions (Table III) as well as the conditions from the LHS design (Table IV).

The identification results with OED and LHS are presented in Tables VI and VII, respectively. We observe that identification with OED consistently results in tighter confidence intervals and better parameter estimates in the case of high sensitivity parameters. This is also illustrated in Fig. 4 that shows relative error in the parameter estimates using the two methods. We observe that relative parameter errors are below 7% in all of the cases when using OED. It is also worthwhile to note that when using OED, the identification algorithm converged in 36 iterations, while 61 iterations were required using the LHS data. Therefore, both the speed and accuracy of parameter estimation is improved with OED.

To underline the importance of the step-by-step identification method presented in Section III, identification results

TABLE VII
IDENTIFICATION RESULTS USING LHS

Parameter	True Value	Estimated Value	95% CI
ω	1000	747.6	2.04×10^6
α_{ca}	0.7	0.689	0.0958
$i_{0,ca}$	3×10^{-7}	3.32×10^{-7}	8.14×10^{-7}
δ_{mb}	15	14.62	4.51
R_{ohm}	8.0×10^{-3}	8.05×10^{-3}	6.45×10^{-3}
$\delta_{GDL,an}$	190	187.6	56.36
$\delta_{GDL,ca}$	190	191.0	22.62

TABLE VIII
SINGLE STEP IDENTIFICATION RESULTS

Parameter	True Value	OED	LHS
ω	1000	1014.1	1581.3
α_{ca}	0.7	0.693	0.703
$i_{0,ca}$	3×10^{-7}	1.14×10^{-7}	3.30×10^{-7}
δ_{mb}	15	23.4	18.19
R_{ohm}	8.0×10^{-3}	2.6×10^{-4}	6.07×10^{-3}
$\delta_{GDL,an}$	190	233.9	212.4
$\delta_{GDL,ca}$	190	216.3	173.7

without such an approach (i.e., identifying all of the parameters using the entire dataset similar to [12], [13]) are given in Table VIII. It is observed that the quality of estimates degrade substantially compared to those in Tables VI and VII.

Overall, the results highlight the significance of the systematic identification approach presented in this paper and underscore the necessity of optimal experimental design for the purpose of parameter identification in fuel cells. As the fuel cell market continues to grow, so does the need for real-time model-based monitoring and control systems that will rely on accurate parameter estimates. It is under such circumstances that the results of this paper and a myriad of related works in the battery literature become even more critical.

V. CONCLUSIONS

A method to optimally design experiments for the purpose of identifying PEM fuel cell model parameters is adapted from the battery literature. The method utilizes the results of local sensitivity analysis to choose a set of experimental operating conditions that maximize the output sensitivity to parameter variations. This, in effect, maximizes the gradient of the residuals that are to be minimized, thereby improving convergence of typical gradient-based least squares algorithms. In addition, a systematic approach for parameterizing models of PEM fuel cells is presented. To identify the model parameters in a step-by-step process, the approach relies on the preceding sensitivity analysis and the fact that different regions of the polarization curve for a fuel cell exhibit different sensitivities to parameter variations. In particular, model parameters are first grouped based on their impact on different regions of the polarization curve. Next, the parameters are identified starting from the data in the kinetic region, and moving towards higher current density data in the mass transport region, allowing for cumulative fitting of

already identified parameters in the process. The framework is tested with a recently developed model and synthetic data generated with the model with known parameter values. The results show that the proposed framework can help with both the accuracy and speed of parameter identification in physics-based PEM fuel cell models.

REFERENCES

- [1] A. Goshtasbi and T. Ersal, "LQ-MPC design for degradation-conscious control of PEM fuel cells," in *Annual American Control Conference*, IEEE, 2019.
- [2] A. P. Schmidt, M. Bitzer, Á. W. Imre, and L. Guzzella, "Experiment-driven electrochemical modeling and systematic parameterization for a lithium-ion battery cell," *Journal of Power Sources*, vol. 195, no. 15, pp. 5071–5080, 2010.
- [3] J. C. Forman, S. J. Moura, J. L. Stein, and H. K. Fathy, "Genetic identification and fisher identifiability analysis of the Doyle–Fuller–Newman model from experimental cycling of a LiFePO₄ cell," *Journal of Power Sources*, vol. 210, pp. 263–275, 2012.
- [4] A. Sharma and H. K. Fathy, "Fisher identifiability analysis for a periodically-excited equivalent-circuit lithium-ion battery model," in *American Control Conference*, pp. 274–280, IEEE, 2014.
- [5] A. M. Bizeray, J.-H. Kim, S. R. Duncan, and D. A. Howey, "Identifiability and parameter estimation of the single particle lithium-ion battery model," *IEEE Transactions on Control Systems Technology*, no. 99, pp. 1–16, 2018.
- [6] X. Lin and A. G. Stefanopoulou, "Analytic bound on accuracy of battery state and parameter estimation," *Journal of The Electrochemical Society*, vol. 162, no. 9, pp. A1879–A1891, 2015.
- [7] L. Zhang, C. Lyu, G. Hinds, L. Wang, W. Luo, J. Zheng, and K. Ma, "Parameter sensitivity analysis of cylindrical LiFePO₄ battery performance using multi-physics modeling," *Journal of The Electrochemical Society*, vol. 161, no. 5, pp. A762–A776, 2014.
- [8] J. Forman, J. Stein, and H. Fathy, "Optimization of dynamic battery parameter characterization experiments via differential evolution," in *American Control Conference*, pp. 867–874, IEEE, 2013.
- [9] M. J. Rothenberger, D. J. Docimo, M. Ghanaatpishe, and H. K. Fathy, "Genetic optimization and experimental validation of a test cycle that maximizes parameter identifiability for a Li-ion equivalent-circuit battery model," *Journal of Energy Storage*, vol. 4, pp. 156–166, 2015.
- [10] S. Park, D. Kato, Z. Gima, R. Klein, and S. Moura, "Optimal experimental design for parameterization of an electrochemical lithium-ion battery model," *Journal of The Electrochemical Society*, vol. 165, no. 7, pp. A1309–A1323, 2018.
- [11] I. V. Zenyuk, P. K. Das, and A. Z. Weber, "Understanding impacts of catalyst-layer thickness on fuel-cell performance via mathematical modeling," *Journal of the Electrochemical Society*, vol. 163, no. 7, pp. F691–F703, 2016.
- [12] P. Dobson, C. Lei, T. Navessin, and M. Secanell, "Characterization of the PEM fuel cell catalyst layer microstructure by nonlinear least-squares parameter estimation," *Journal of the Electrochemical Society*, vol. 159, no. 5, pp. B514–B523, 2012.
- [13] B. Carnes and N. Djilali, "Systematic parameter estimation for pem fuel cell models," *Journal of Power Sources*, vol. 144, no. 1, pp. 83–93, 2005.
- [14] A. Goshtasbi, B. L. Pence, and T. Ersal, "Computationally efficient pseudo-2D non-isothermal modeling of polymer electrolyte membrane fuel cells with two-phase phenomena," *Journal of the Electrochemical Society*, vol. 163, no. 13, pp. F1412–F1432, 2016.
- [15] A. Goshtasbi, B. L. Pence, and T. Ersal, "A real-time pseudo-2D bi-domain model of PEM fuel cells for automotive applications," in *ASME Dynamic Systems and Control Conference*, p. V001T25A001, 2017.
- [16] B. F. Lund and B. A. Foss, "Parameter ranking by orthogonalization—Applied to nonlinear mechanistic models," *Automatica*, vol. 44, no. 1, pp. 278–281, 2008.
- [17] S. Wright and J. Nocedal, "Numerical optimization," *Springer Science*, vol. 35, no. 67–68, p. 7, 1999.
- [18] C. Wild and G. Seber, "Nonlinear regression," 1989.